CLM-P 127

United Kingdom Atomic Energy Authority

RESEARCH GROUP

Preprint

POWER CROWBAR OF LOW INDUCTANCE CAPACITOR BANKS USING ATMOSPHERIC SPARK GAPS

N. R. McCORMICK
D. MARKINS
L. FIRTH

Culham Laboratory
Abingdon Berkshire

1966

UNCLASSIFIED
(Approved for publication)

CLM-P127

POWER CROWBAR OF LOW INDUCTANCE CAPACITOR BANKS USING ATMOSPHERIC SPARK GAPS

by

N.R. McCORMICK
D. MARKINS
L. FIRTH

(Submitted for publication in Proc.Inst.Elec.Engrs.)

ABSTRACT

An atmospheric simultaneously-overvolted sparkgap has been developed for crowbar duty in fast capacitor banks. The sparkgap utilises movement of the arc away from a back-strap earth conductor to reduce the rate of electrode erosion in the breakdown region, giving reliable operation for some thousands of discharges at an ampere-seconds rating of 4.5 coulombs. A powered-crowbar test rig comprising 28 separately switched circuits has been constructed to provide experience in the design and operation of multiple parallel circuits, such as would be required for a large capacitor bank.

U.K.A.E.A. Research Group,
Culham Laboratory,
Abingdon,
Berks.

November 1966 (D/S)

C O N T E N T S

1. INTRODUCTION

High-voltage capacitor banks have been widely used in recent years for the production of high-current transient discharges for research on high-temperature plasmas generally, and in particular for research directed towards the achievement of controlled nuclear fusion[1]. Usually the discharge of the capacitor bank is only lightly damped in order to achieve a high peak current, and experimental observation of the plasma is limited in duration to rather less than one half period of oscillation, as in Fig.1(a). The duration of undirectional current flow may be extended by clamping the capacitor voltage at zero, when the current is approximately at its peak value; in effect this traps energy in the load inductance and, following clamp, the load current falls exponentially. "Clamp" is also known as "crowbar" from the analogy of throwing a crowbar across live terminals to provide a short circuit. In passive clamp a low-inductance short circuit is switched across the load at voltage zero, as in Fig.1(b). In active (powered) clamp the current is maintained for a longer time by feeding further energy into the load; commonly this is accomplished by including a series high-capacitance, low-voltage capacitor in the clamp circuit as in Fig.1(c), where the clamp capacitor need only be charged to a sufficient voltage to overcome the resistive voltage drop at peak current.

The clamp switch must withstand a large fraction of the total bank voltage immediately after the start switch closes, and yet must trigger reliably at zero voltage. Moreover, the clamp inductance must be small by comparison with the load inductance, which can be a stringent requirement in some experiments where the load inductance may only be a few nonohenries. The total peak current capability required of the clamp-switch system may be some tens of megamperes, and the ampere second requirement some thousands of coulombs. As in the case of start switches, parallel switched circuits are essential to reduce switch loading and stresses, whilst also permitting a higher inductance per circuit. The time precision in closing of individual switches must be of the order of a tenth of a μsec.

Various types of switch have been considered for clamp duty[2], including vacuum sparkgaps[3-8], low-pressure mercury-vapour tubes[9,10], mechanical switches[11], and recently a solid dielectric switch has been developed[12-16]. Usually atmospheric sparkgaps can be triggered only down to about half the maximum working voltage, unless a series impedance is included across which a fast overvoltage can be developed[1]. However, in the simultaneously-overvolted mode[1,17] the 3-electrode sparkgap may, by suitable choice of gap ratio, be set to trigger at any voltage down to zero, although with only a small working range of voltage. The atmospheric sparkgap has several advantages for use as a high-power high voltage switch: the time precision in operation is of the order of ten nanoseconds, the gap is self healing, and is not temperature sensitive. By comparison with some other switches the charge-handling ability is small; but this can be overcome by using more switches in parallel, with consequently a higher permitted inductance per switch and lower stresses. Trigger systems for generating several hundred fast high-voltage pulses have already been used in capacitor banks[18], and could be extended further if necessary.

This work started as a general investigation of the characteristics of the simultaneously-overvolted atmospheric sparkgap as a switch for clamp, or crowbar, duty. It was extended into a design study for a clamp system for the 1-megajoule capacitor bank for thetatron research in nuclear fusion at Culham[18].

2. THE SIMULTANEOUSLY-OVERVOLTED MODE OF OPERATION OF A 3-ELECTRODE SPARKGAP

The circuit of Fig.2(a) represents a capacitor C charged to voltage V_W and switched by a 3-electrode approximately uniform-field sparkgap. Under static conditions the common electrode of the sparkgap is held at a voltage intermediate between the two outer electrodes such that the voltages across the component gaps are in the ratio of their gap lengths, and the component gaps are equally stressed. If the trigger pulse $V_T(t)$ is of opposite polarity to V_W the stress in gap 1 will increase with V_T whilst the stress in gap 2 will fall to zero before increasing in reverse direction. For operation in the swinging-cascade mode two conditions restrict the choice of the gap ratio $q = \ell_2/\ell_1 + \ell_2$: first, gap 1 must

breakdown before gap 2, and secondly, gap 2 must breakdown on the subsequent rise of voltage across the capacitor C. With small damping and suitable choice of L and C the voltage across C will overshoot V_W, which in effect increases the working voltage range of the gap. The voltage waveform at the common electrode is of the form shown in Fig.2(b); the voltage swing on the common electrode and the cascade breakdown of the two gaps gives rise to the name given to this mode of operation. With suitable choice of gap ratio and circuit parameters the sparkgap will operate in this mode down to about one half the maximum working voltage.

In the swinging-cascade mode, breakdown of gap 1 occurs due to an overvoltage caused directly by the trigger pulse and gap 2 subsequently, due to an overvoltage largely independent of the trigger pulse. For a particular value of V_W, q may be chosen so that the trigger pulse causes both gaps to reach breakdown simultaneously: Fig.2(c) represents the trigger-electrode waveform in this mode, called the simultaneously-overvolted mode. The relationship between the working voltage V_W and the value of q for simultaneous breakdown of the two component gaps may be obtained as follows. If the trigger voltage at breakdown is V_{TB}, and the corresponding breakdown voltages across gaps 1 and 2 are V_{1B} and V_{2B}, then:

$$V_{1B} = (1 - q)\, V_W + V_{TB}$$

$$V_{2B} = V_{TB} - q\, V_W$$

from which it follows that:

$$\frac{V_W}{V_{1s} + V_{2s}} = (1 - q)\, f(\dot{E}_1) - q\, f(\dot{E}_2)$$

where V_{1s} and V_{2s} are the static breakdown voltages of gaps 1 and 2, assumed proportional to ℓ_1 and ℓ_2. The function $f(\dot{E}) = E_B/E_S$ is an impulse ratio for approximately linearly-rising overvoltages, which has been measured over a relevant range of gap lengths at atmospheric pressure[1]. In the obvious case when $q = \frac{1}{2}$ and the gaps are identical, simultaneous breakdown will occur when $V_W = 0$, which is the required condition for duty as a clamp switch.

In the simultaneously-overvolted mode, if one gap should breakdown slightly early it will reduce the overvoltage, i.e. chop the voltage, across the other. An early breakdown of one gap could occur either because of dimensional manufacturing tolerances, or because of some small residual steady voltage across the gap. If the available overvoltage should collapse instantaneously there would be zero working tolerances. In practice this does not occur because of the finite rate of fall of spark-channel resistance in the early gap[19,20], and because of the finite inductance of the early gap and its connections combined with circuit stray capacitances. As a consequence the overvoltage across the late gap may be maintained sufficiently for the ionisation processes there - which will have already nearly reached breakdown - to continue to completion. In effect this gives some tolerance in gap ratio for a fixed working voltage, or voltage range for a fixed gap ratio. The working tolerances increase with $V_T^{\cdot}$: the higher the value of $V_T^{\cdot}$, the higher the overvoltage at breakdown of the early gap, and the more overvoltage available to breakdown the late gap.

3. APPLICATION AS A CLAMP SWITCH

3.1. Circuits

Fig.3 shows the voltage and current relationships in a simplified passive-clamped capacitor discharge circuit having no resistive losses. When the start switch S_1 is closed, the current i_3 in the load L_3 rises sinusoidally to the peak value $I_p = V_B \sqrt{\frac{C}{L_1+L_3}}$ in the 1/4-period $\frac{\pi}{2}\sqrt{C(L_1+L_3)}$, in which time the voltage at all points in the circuit falls to zero. S_2 is then closed. Subsequently, the load current 1_3 has the same peak value I_p , but there is superimposed a ripple of amplitude $I_p \times \frac{L_2}{L_2+L_3}$ about the mean value $I_p \times \frac{L_3}{L_2+L_3}$, with a reduced period $2\pi\sqrt{L_1 + \frac{L_2 L_3}{L_2+L_3}}$. The current i_1 oscillates with the same peak amplitude, I_p , as before, and with the reduced period. The clamp current i_2 has a (1-cosine) waveform of mean amplitude $I_p \times \frac{L_3}{L_2+L_3}$ and period as for i_2, and i_3 . For small ripple the clamp inductance L_2 must be small by comparison with the load inductance L_3 . In the extreme case when $L_3 = 0$ the

closing of S_2 completely isolates the start and load circuits: the current i_2, then oscillates with peak amplitude I_p and period $2\pi\sqrt{L_1C}$, and the load current i_3 remains steady at I_p. The effect of circuit resistance is to damp the oscillatory component of the currents and to cause the mean load current to fall exponentially.

If, for powered clamp, a capacitor C_2 is inserted in series with L_2, generally $C_2 \gg C_1$, and closing S_2 effectively increases the discharge capacitance from C_1 to C_2. A new discharge waveform is thus defined, with increased period and damping, and with the initial conditions set by the current I_p in the load inductance and by the capacitor voltage V_2. It may be best to fix V_2 high enough to cater for all forseeable load resistances, and to adjust the waveform after clamp by means of a series damping resistor in the clamp circuit.

All measurements were carried out using the basic circuit of Fig.4, in which both start and clamp switches are connected at the input to the main cables feeding the load. C_1 is the start capacitor, S_1 and S_2 the start and clamp switches, L_F the load inductance chosen to represent per circuit a typical load inductance of a large capacitor bank, and R_d a resistor to damp switching surges which otherwise would make many transits of the main cable. Whilst R_d should heavily damp transients in the main cable, it should be high enough to avoid serious damping of the main discharge; this is not difficult since the effective frequency of the unwanted transients is much higher than the main discharge frequency. Fig.5 shows the detailed circuit for the simultaneously-overvolted gap as the clamp switch S_2. Before S_1 closes all the electrodes are at zero voltage. When S_1 closes voltage transients across S_2 are graded by the capacity divider C_xC_x so that, prior to triggering, the two series gaps are equally stressed. The value of C_x must be large enough to swamp circuit stray capacitances. The series sparkgap G_s isolates the capacity divider from the trigger-cable impedance, and also acts as a pulse-sharpening switch, and for this latter reason should be pressurised. G_s has an irradiating gap to reduce the statistical jitter in breakdown. Capacitor C_y assists pulse sharpening and

ensures adequate irradiating current in G_S . The common (trigger) electrode of the clamp sparkgap also has an irradiating gap, located inside the electrode, which illuminates the main gap electrodes through small-diameter axial holes. Clamp capacitors can be included as shown dotted in Fig.5; connection to the capacitors would probably be by parallel-strip transmission line, for low inductance.

Some simplification of the circuit can be achieved, as shown in Fig.6, by omitting the series sparkgap G_S ; in this case the trigger electrode must be maintained at a steady d.c. bias of one half the peak voltage across the clamp switch, to equalise the peak stresses in the two component gaps. For economy in trigger-pulse amplitude, the trigger-pulse polarity should be the same as the main bank voltage. This circuit has the disadvantage that it cannot be operated unclamped without disconnecting the clamp switches, because they would break down in an uncontrolled manner on the second quarter cycle of the discharge.

3.2 Sparkgap details

The simultaneously-overvolted sparkgap operating as a clamp switch has been demonstrated successfully with various mechanical configurations, but this description is confined to the one developed from the existing atmospheric swinging-cascade gap used in the megajoule thetatron capacitor bank[18]. A cross-section of the complete start-clamp sparkgap assembly is shown in Fig.7. The original swinging-cascade gap has four electrodes moulded in 6-inch diameter epoxy holders, spaced with annular epoxy rings, each provided with six small holes for ventilation to the atmosphere. One of the two centre electrodes is the trigger electrode with an internal irradiating gap, and the other an isolating electrode. Connection to the two outer electrodes is by flexible polythene-insulated coaxial cable with the earth braids stripped back and clamped to the earth tray. In the combined sparkgap the output electrode of the swinging-cascade section has been made double-sided and the further two electrodes of the simultaneously-overvolted section added axially in line with the swinging-cascade electrodes. The main cable feeding the load is formed by four 50-ohm coaxial cables in parallel, which feed into the sparkgap above the earth-

return tray, passing through the electrode holder of the clamp gap : there is then a magnetic field, after clamp, acting to blow the arc in the clamp gap away from the earth tray. The clamp-gap electrodes are 3/4-inch radius in the breakdown region, for 1-cm gap lengths, giving an approximately uniform field in the breakdown region. The electrodes are conically shaped in a direction perpendicular to the earth tray to permit movement of the arc away from the breakdown region without an appreciable increase in arc length. To accommodate the electrodes and movement of the arc channel, the arc chamber is extended in a direction perpendicular to the earth tray: suitable dimensions were found using streak and framing-camera photographs of the moving arc, confirmed by empirical tests.

The irradiating sparkgap with its by-pass resistor and the series pressurised gap G_S are contained in a single assembly, which fits into the trigger-electrode moulding with the irradiating gap correctly aligned opposite the axial holes in the trigger electrodes. The sparkgap G_S is pressurised with nitrogen at 50 lb./sq. in.

The end termination of the clamp sparkgap is an epoxy resin moulding containing a parallel-plate feedout to a termination beneath the cables, which connects to a parallel-plate line to the clamp capacitors.

3.3. Performance

Preliminary tests were made using several different arrangements of sparkgaps and circuits to test particular features of operation, but finally the work was directed towards the development of a powered clamp system that could be applied to the 1 MJ thetatron bank. The details of the final circuit arrangement are shown in Fig.8, where the starting components and circuit are identical to those used in the megajoule bank. The load inductance of 4.5 μH corresponds to a load of 10 nH for the complete bank of 448 parallel circuits. Trigger pulses for the test circuit were generated by the discharge of d.c.-charged coaxial cables through pressurised low-inductance swinging-cascade sparkgaps triggered from 5C22-type hydrogen thyratrons. The delay between the start and clamp trigger pulses was introduced at low voltage level in the pulse-generators

feeding the thyratrons. The tests were concerned with measurement of the working range in the timing of the clamp trigger pulse relative to the closing of the start switch, in order to assess whether the simultaneously-overvolted gap would have sufficient working tolerances and would be sufficiently reliable for use in a large system containing several hundred gaps. It was necessary to relate the working timing range to the rate of rise of trigger-pulse voltage and to mechanical tolerances in gap dimensions; and also to measure the change in characteristics with use and to observe the incidence of occasions of spurious breakdown or failures to trigger.

The timing range, which is used as an indication of the working voltage range of the simultaneously-overvolted gap, will depend on the rate of change of capacitor voltage in the region of voltage zero, and hence on the period of the oscillatory discharge; a reasonable target is ± 10% of the 1/4-period. The timing range was measured by changing the delay between the initiating pulses to the hydrogen thyratrons in steps of 0.1 μsec, and by observing the voltage waveform across the clamp switch at each step to detect incorrect operations or failures: this requires that the jitter in the chain of pulse generators leading to the production of the trigger pulses fed to the sparkgaps, and in the operation of the start gaps, should be appreciably less than the step interval. Nine waveforms were recorded (on a single polaroid frame) at each delay setting: when faults were observed the edge of the range was investigated in greater detail with a larger number of records. Fig.9 shows voltage waveforms measured across the clamp sparkgap at the edge of the working timing range. Two waveforms show incorrect operation, in which only one of the two series gaps has broken down under the applied trigger pulse and the second one has broken down under direct overvoltage on the second quarter cycle. Measurements of the timing range required a large number of discharges and in the course of these, experience was accumulated on the reliability of the system. It was found that with a 1/4 period of 6 μsec the edges of the range were defined to within 0.2 μsec (the range might typically be 2 μsec), and within the working range there were no spurious breakdowns or failures to operate. The gap settings

of course must be large enough to withstand any transient voltages in excess of V_W with a suitable safety factor. The maximum working voltage was 40 kV. With the damping resistor R_D connected transients did not exceed 20% above V_W, and each component gap of the simultaneously-overvolted gap had a static breakdown voltage of 30 kV, giving a nominal safety factor of 25%.

Regarding our lack of observed spurious breakdowns (of the clamp gap) it is reasonable comment that atmospheric sparkgaps do occasionally breakdown below their normal static breakdown stress (they are not unique in this respect among high-voltage switches). For example, it is common to find some spurious breakdowns of start gaps when charging a bank after a period out of use (although in regular use such occurrences should be a comparative rarity). The simultaneously-overvolted gap cannot expect to be immune. Anomalously-low breakdown voltages in start gaps should be self-clearing due to breakdowns during charging, whereas the clamp gaps are not stressed before the start gaps operate, which makes ageing the clamp gaps difficult. There will be less tendency for the clamp gaps to breakdown, however, because their stress is transient and of only a few microseconds duration (in clamped operation), and perhaps this explains the lack of observed spurious breakdowns in our tests. It would be unwise to rely on this in a large bank, and precautions must be taken to ensure that spurious breakdowns do not couple transient voltages into other circuits sufficient to initiate the uncontrolled breakdown of other sparkgaps.

Fig.10 shows the measured timing range as a function of $\dot{V}_T$. This curve was one of the preliminary results before conditions were optimised and shows the type of relationship rather than the detailed performance of the final design. $\dot{V}_T$ is the rate of rise of trigger-pulse voltage at breakdown measured at the trigger-cable termination.

Fig.11 shows the increase in lengths of the two component gaps caused by electrode erosion as a function of the number of discharges, showing the reduction in the rate of electrode erosion obtained through the use of arc blow-out. This test was made using an experimental gap in which the adjacent current-carrying

leads could be arranged symmetrically to prevent arc blow-out. As would be expected, the increase in gap length is very nearly the same for the two component gaps, so that there should be no significant shift in the timing range until gross change in their contours modifies the electric field distribution. This point was not reached in these tests and it was checked that the limits to the timing range at the end of the run were unaltered within 0.2 μsec. Using magnetic blow out of the arc it should be possible, from these results, to obtain a life of 10^4 discharges without reconditioning or replacement of electrodes if the charge passed per shot is limited to less than 4.5 coulombs.

Fig.12 shows the timing range of a simultaneously-overvolted gap as a function of the gap ratio q for both bank polarities and positive trigger polarity, with $\dot{E_T}$ approximately 4 kV/cm/nsec. These curves indicate a permissible tolerance in gap lengths of ± .005" for a working timing range of 1 μsec in a 1/4-period of 7 μsec. The gap dimensions were the final ones, but there was no intentional irradiation and the gap was completely open to the atmosphere. Measurements at this time showed that the main gaps apparently did not need irradiation: subsequently the gaps were enclosed to reduce the noise, and then failed to operate, indicating that irradiation had occurred accidentally, probably by reflection (sharp points connected to the trigger electrode were positioned adjacent to the gaps without success). Fig.13 shows the operating ranges for the final sparkgap design with irradiation, with the trigger pulse generator charged either to 100 kV or 115 kV, with and without irradiation of the series gap G_s .

Fig.14 shows a streak-camera photograph of the arc in the clamp gap. The arc travels out to the end of the electrodes and must then increase rapidly in length for any further movement; there comes a point when conditions are more favourable for the formation of a second channel at a shorter gap length.

4. A POWERED-CLAMP TEST RIG

A test rig comprising 28 parallel circuits has been constructed to test engineered components and to enable problems arising from the complexity of multiple circuits to be met without the urgency attached to the commissioning of a large bank. It is large enough, however, to form a useful current-discharge source for driving plasma physics experiments.

A schematic diagram of the circuit is shown in Fig.15. Each discharge circuit is identical to that in Fig.8, arranged horizontally on a timber rack structure, 14 circuits per rack, with the sparkgap central and the start and clamp capacitors feeding into it from either side, as can be seen in the view between racks in Fig.16. The normal working voltage range of the start capacitors is 30-40 kV. The clamp capacitors are always charged to 4 kV and the discharge waveform is adjusted by varying the value of the series damping resistors. A 20 μF capacitor across the clamp sparkgap termination prevents an excessive voltage rise at that point from trigger-pulse feed through, or in the event of a fault.

The start and clamp sparkgaps have independent trigger systems initiated by low-level pulses with a variable delay between them. Each trigger system is capable of expansion into a cascade system generating several hundred pulses, similar to that proved in the megajoule thetatron bank. The start system operates at identical voltages to those used previously, so it was not necessary to prove it again, and a single master generator produces 28 output pulses. The clamp trigger system operates at the higher voltage of 100 kV and comprises all the essential features of a larger system, to prove the reliability: a master generator produces 16 output pulses, one of which triggers a sub-master generator producing 28 output pulses; the clamp trigger system therefore contains the elements of a cascade system capable of producing 448 output pulses.

All the trigger-pulse generators are pulse-charged in about 1 μsec to reduce the probability of spurious breakdown of the sparkgaps. The two systems are charged from marx generators triggered from blümlien-type pulse generators: each blümlien circuit produces pulses to trigger its associated marx generators and an additional pulse which is delayed by 1 μsec (in coaxial cable) and used to trigger the master trigger-generator sparkgap at the peak of the charging waveform. Wavetail resistors connected across the marx generator outputs give decay time constants of 15 μsec if, in the course of testing, the trigger system is not triggered.

The trigger-pulse generators are similar to those used previously in the megajoule thetatron bank,[18] except that the clamp trigger system uses larger-diameter cables because of the higher voltage. Two sets of radially-connected coaxial cables are switched together by a low-inductance pressurised triggered swinging-cascade sparkgap: the sparkgap discharges the pulse-charged cables (trigger-discharge cables) into the output cables (trigger-pulse cables). The sparkgaps use compressed SF_6, at 25 lb./sq.in. for the start system and 45 lb./sq.in. for the clamp system. Sparkgap dimensions are identical for all generators, with details of the earthed cable connecting ring adjusted to suit the type and number of cables. The effective rate of rise of trigger-pulse voltage measured at an open-circuit cable termination is approximately 5 kV/nsec, rising to 100 kV.

For all the initial tests the collector cables were 28 ft. long, as in the megajoule bank. Fig.16(a) shows waveforms corresponding to the discharge of 1 rack into a short circuit across the collector output, for both the unclamped oscillatory discharge and the passive-clamped discharge. Referring to the equivalent circuit of Fig.16(b): the value of $(L_1 + L \text{ cables})$ may be calculated from the period of oscillation of the unclamped discharge; $\left(L_1 + \frac{L_2 \; L \text{ cables}}{L_2 + L \text{ cables}}\right)$ from the period of oscillation of the capacitor voltage after clamp; and $\left(\frac{2L_2}{L_2 + L \text{ cables}}\right)$ from the ratio of ripple amplitude on the current waveform after clamp, to the peak current. The waveforms shown give the values $L_1 = 30$ nH, $L_2 = 13$ nH and L cables = 56 nH, per rack; or $L_1 = 420$, $L_2 = 180$, and L cables = 780 nH per circuit. The extra

inductance of the clamp capacitors and the associated connections for powered clamp may be estimated as an additional 50 nH per circuit, 3.5 nH per rack. Fig.18 shows waveforms of current for the oscillatory, passive-clamped and active-clamped discharge of 1 rack into a 170-nH coil. Since the above results were taken the second rack has been commissioned to enable both racks to be used to power experiments in plasma physics. The main cables are now 7-ft. long, and a 20-nH load coil has been attached. Current waveforms are shown in Fig.19.

5. CONCLUSIONS

It has been demonstrated that an atmospheric 3-electrode sparkgap operating in the simultaneously-overvolted mode can be used as a clamp switch in large capacitor banks with acceptable working tolerances. Low overall clamp inductance and high effective ampere-second and peak current capability would follow through the use of many parallel switches. All the essential engineered features of a cascade trigger system for a large capacitor bank, comprising several hundred parallel circuits, are under test in a 28 circuit rig currently being used to power theta-pinch experiments in plasma physics.

6. ACKNOWLEDGEMENTS

Early work on the simultaneously-overvolted mode was initiated by R.A. Fitch at AWRE, Aldermaston, and carried out in collaboration with the authors. Numerous colleagues have assisted in various aspects of the present work, notably R.J. Hucklesby on the mechanical design, and P. Roberts and T. Quayle on the charging, protection and control circuits.

The paper is published by permission of the Director of Culham Laboratories of the Atomic Energy Authority, where the work formed part of a programme of theta-pinch research.

7. REFERENCES

1. FITCH, R.A., and McCORMICK, N.R. 'Low inductance switching using parallel sparkgaps', Proc. IEE, 1959, 106 A, Suppl. 2, p.117.

2. HANCOX, R. 'Low pressure gas discharge switches for use in fusion experiments', Proc. IEE 1964, 111, p.203.

3. HAGERMANN, D.C. and WILLIAMS, A.H. 'High-power vacuum sparkgap', Rev. Sci. Instrum., 1959, 30, p.182.

4. BAKER, W.R. 'High voltage, low inductance, switch for megampere pulse currents', Rev. Sci. Instrum., 1959, 30, p.700.

5. JOHANSON, R.B., and SMARS, E.A. 'A low-pressure spark gap switch with wide voltage range', Proc. 5th Int. Conf. on ionisation phenomena in gases, 1961, p. 1040.

6. KOLB, A. 'Clamp system for the Pharos 2 MJ energy storage capacitor bank', Report of NRL progress, 1965, April, p.11.

7. YOUNG, M.P. '20 kV vacuum switches for crowbar applications', Proc. 3rd symposium on engineering problems in thermonuclear Research, Munich, 1964. p.115.

8. YOUNG, M.P. 'Pharos crowbar system', Proc. 1965 symposium on engineering problems of controlled thermonuclear research, Livermore, p.57

9. KNIGHT, H. de B., HERBERT, L., and MADDISON, R.C. 'The ignitron as a switch in high-voltage heavy-current pulsing circuits', Proc. IEE, 1959, 106A, Suppl. 2, p.131.

10. KEMP, E.L., and QUINN, W.E. 'The power crowbar energy system for Scylla IV', Proc. 3rd symposium on engineering problems in thermonuclear research, Munich, 1964, p.70.

11. ROGERS, P.J. "A fast mechanically-closed switch", Proc. 3rd symposium on engineering problems in thermonuclear research, Munich, 1964. p.146.

12. ALSTON, L.L., et.al. 'A solid dielectric switch', Proc. 3rd symposium on engineering problems in thermonuclear research, Munich, 1964, p.153.

13. FRIEDRICH, A.J. 'A solid dielectric trigatron for crowbar', Proc. 3rd symposium on engineering problems in thermonuclear research, Munich, 1964. p.162.

14. ALSTON, L.L. et al. 'Some experiments on a high-power closing switch with polythene as the main dielectric', Proc. IEE, 1965.

15. JAMES, T.E., HARRIES, K, and MEDFORD, R.D. 'Development of fast 100 kV 1 MA solid dielectric switches and associated triggering studies', Proc. 1965 symposium on engineering problems of controlled thermonuclear research, Livermore, p.77.

16. BAYES, D.V., HUCKLESBY, R.J., and WARD, B.J. 'A passive crowbar for the 1 MJ thetatron bank using 32 solid dielectric switches in parallel', Proc. 4th symposium on engineering problems in thermonuclear research, Rome, 1966.

17. FITCH, R.A., and McCORMICK, N.R. 'The modes of operation of a cascade spark-gap for precision switching', Proc. 4th Int. Conf. on ionisation phenomena in gases, Uppsala 1959, p.463.

18. McCORMICK, N.R. 'A 1-megajoule Low-inductance capacitor bank for nuclear fusion research', Proc. I.E.E.

19. STREET, J.C., and BEAMS, J.W. 'The fall of potential in the initial stages of electrical discharges', Phys. Rev. 1931, 38, p.416.

20. FLETCHER, R.C. 'Impulse breakdown in the 10^{-9} second range of air at atmospheric pressure', Phys. Rev. 1949, 76, No.10, p. 1501.

ADDENDUM TO CLM - P 127

Fig. 5 The capacitor shown C_z should read C_{CL}

Fig. 9 The time-base duration of the oscilloscope traces is 16 μsec

Fig. 14 The figure caption should read:

Streak-camera record showing arc movement in the clamp gap

The time scale corresponding to the distance AB = BC = CD of the streak photograph is 70 μsec

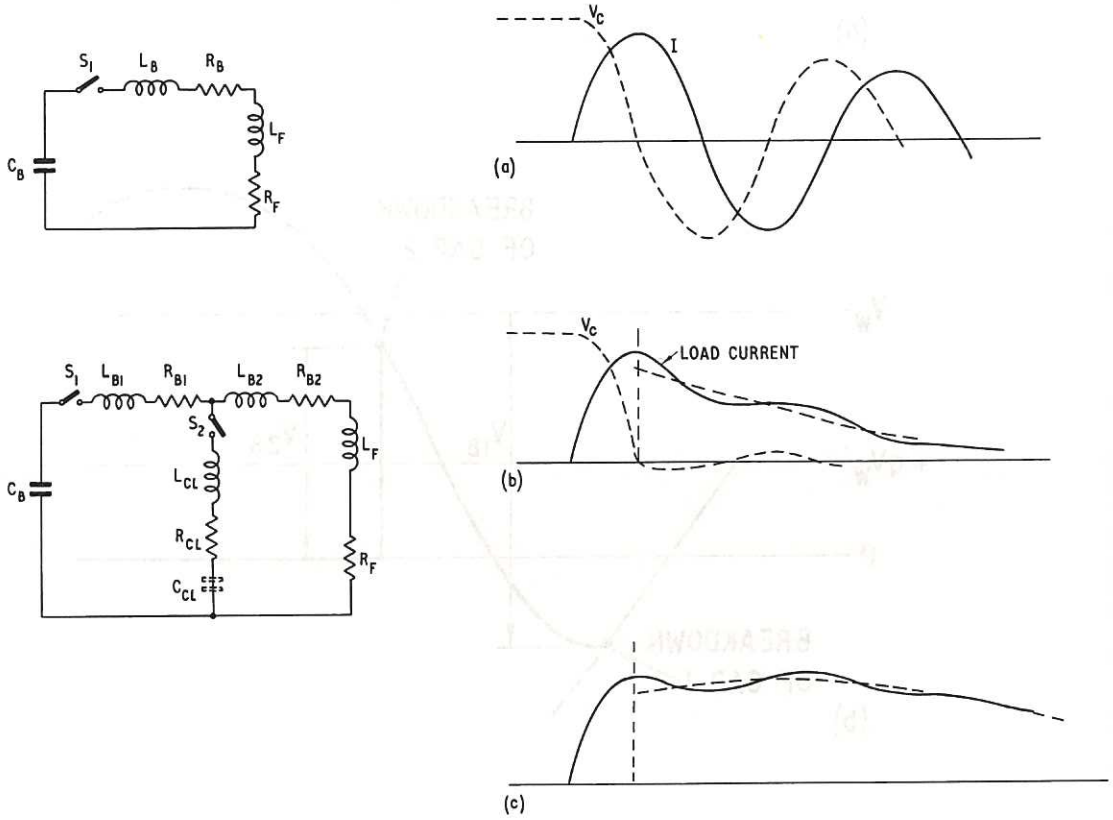

Fig. 1 (CLM-P 127)

Simplified circuit diagram and current waveforms for a capacitor-bank discharge: (a) unclamped: (b) passive clamp: (c) powered clamp

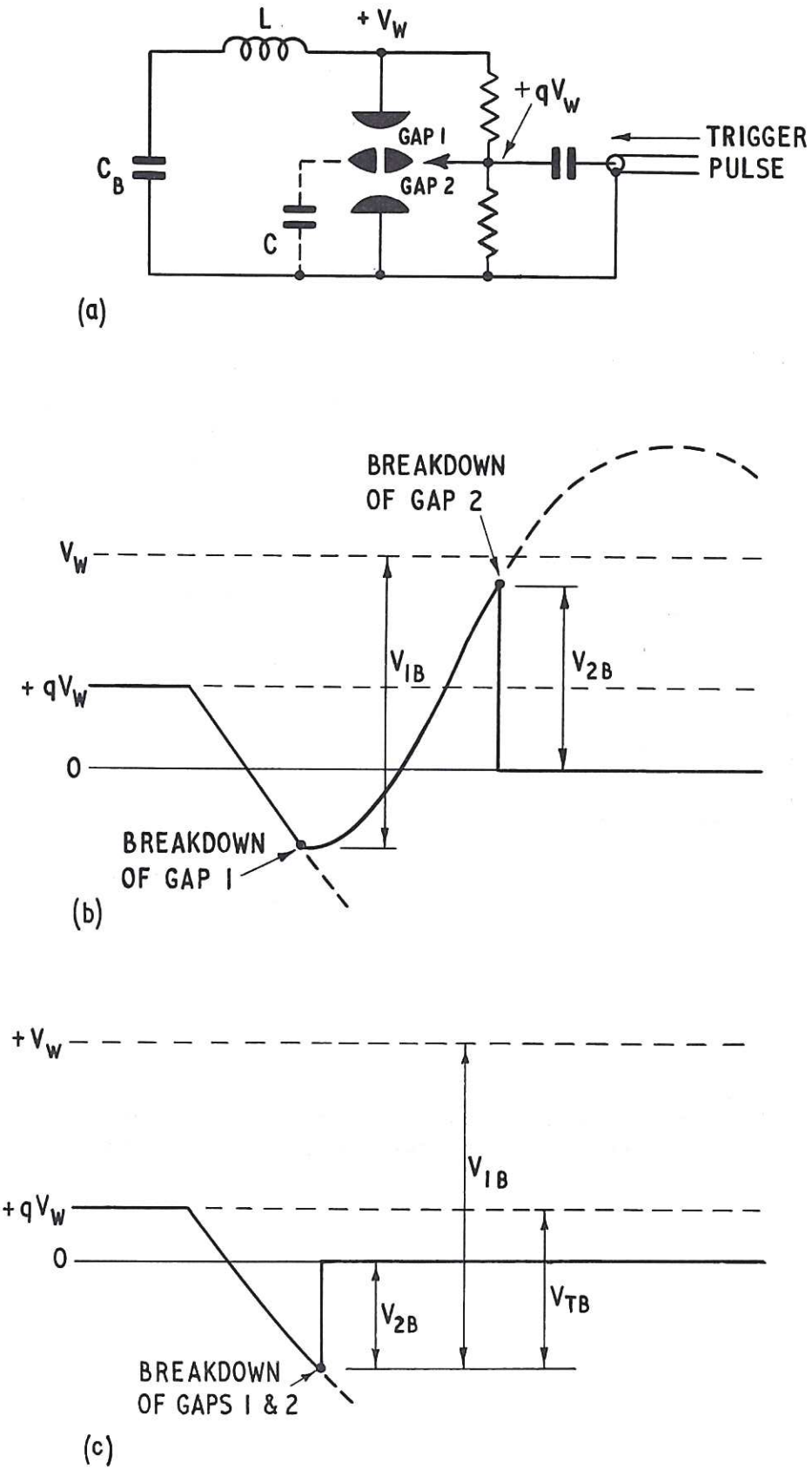

Fig. 2 (CLM-P 127)

The 3-electrode triggered spark gap: (a) circuit diagram: (b) trigger-electrode waveform in swinging-cascade mode: (c) trigger-electrode waveform in simultaneously-overvolted mode

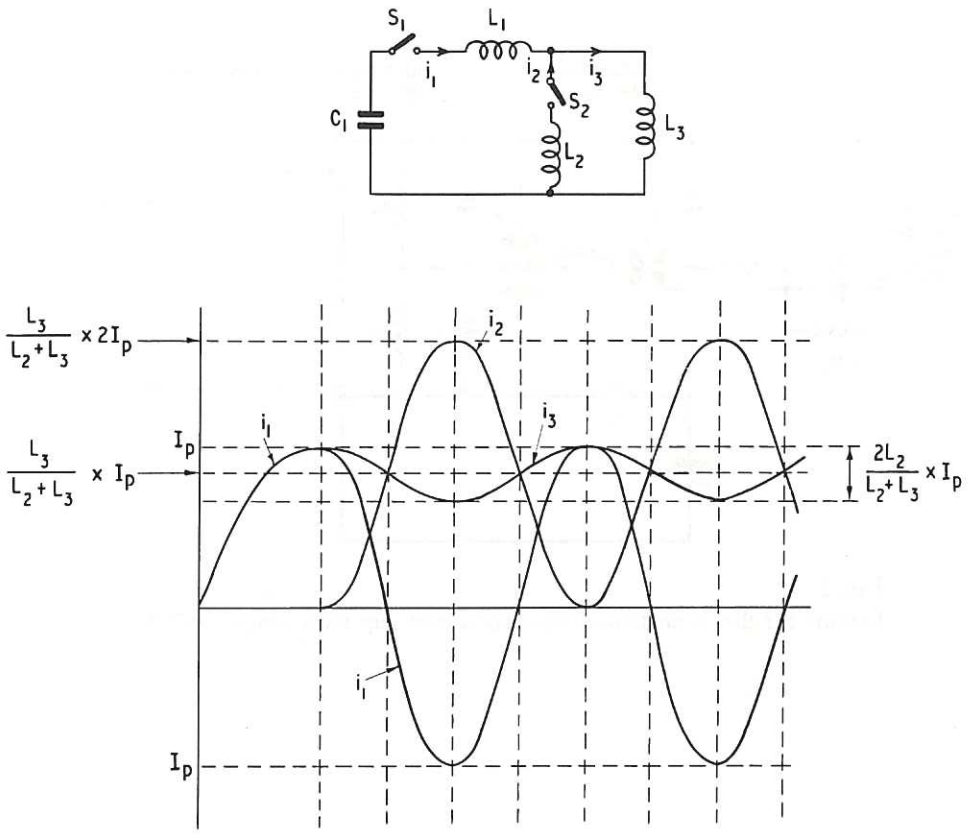

Fig. 3 (CLM-P 127)
Lossless passive clamp circuit and waveform

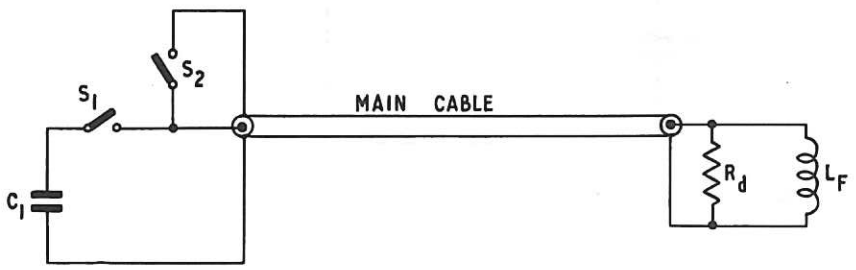

Fig. 4 (CLM-P 127)
Basic circuit used in the study of the characteristics of the simultaneously-overvolted gap as a clamp switch

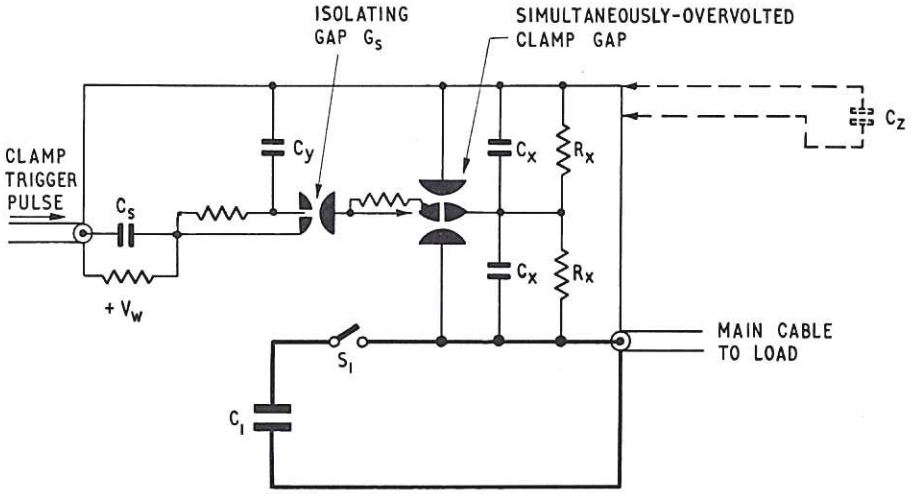

Fig. 5 (CLM-P 127)
Circuit for the simultaneously-overvolted gap as a clamp switch

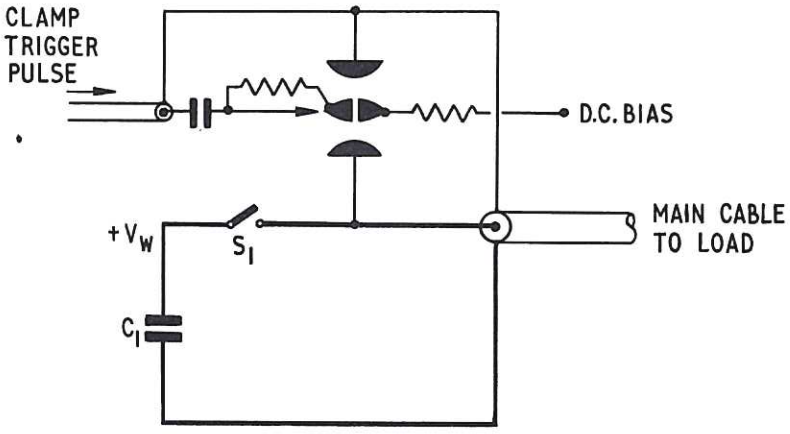

Fig. 6 Alternative passive-clamp circuit (CLM-P 127)

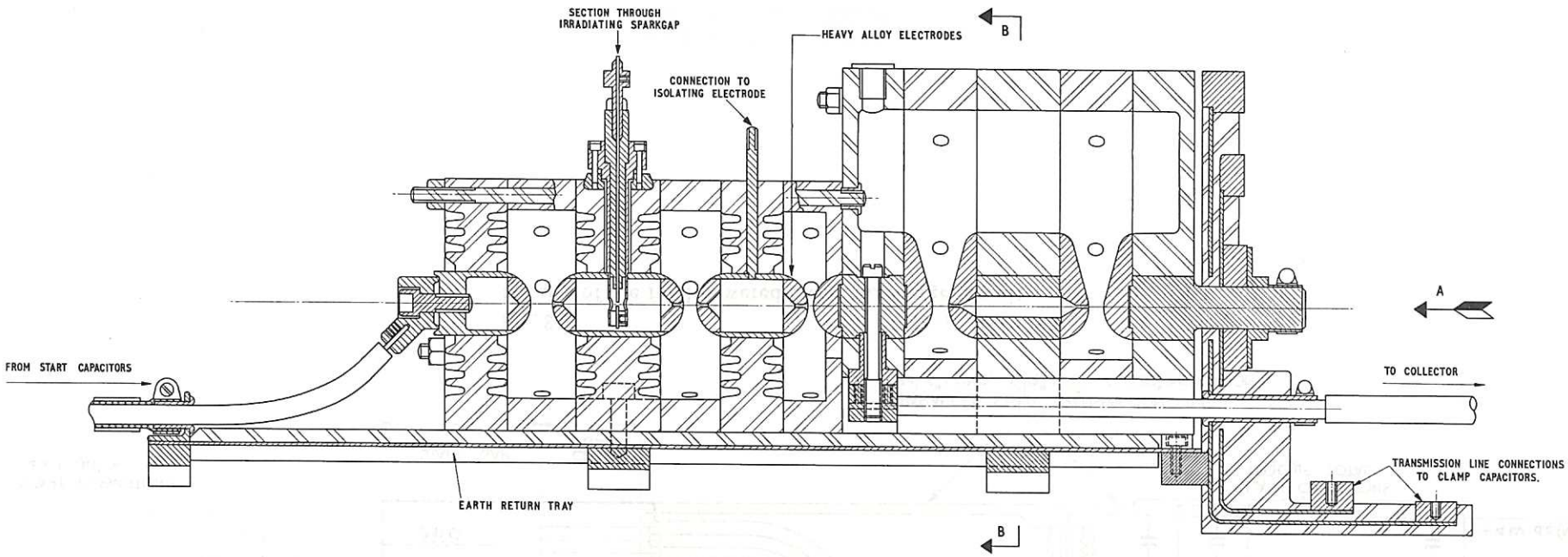

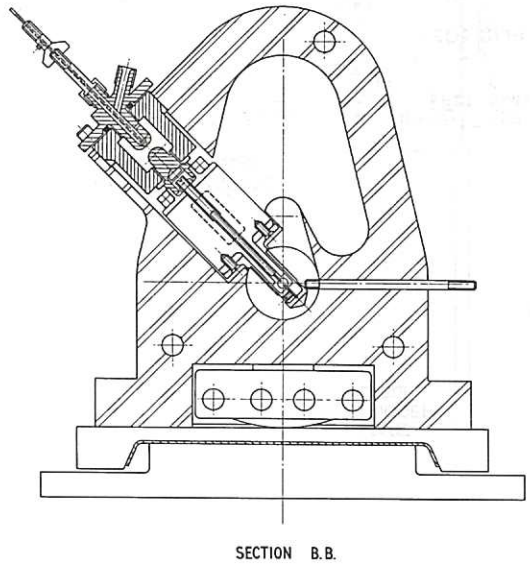

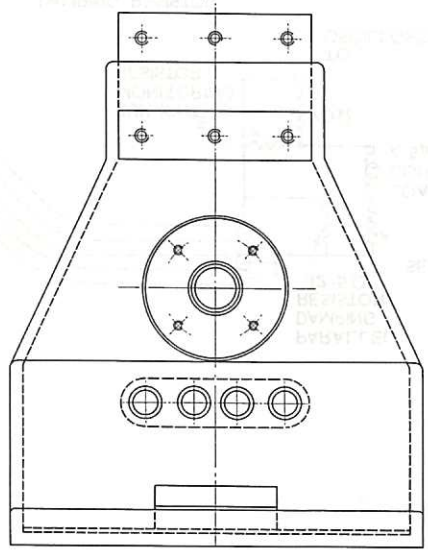

Fig. 7 (CLM-P 127)
Mechanical details of the combined start-clamp switch

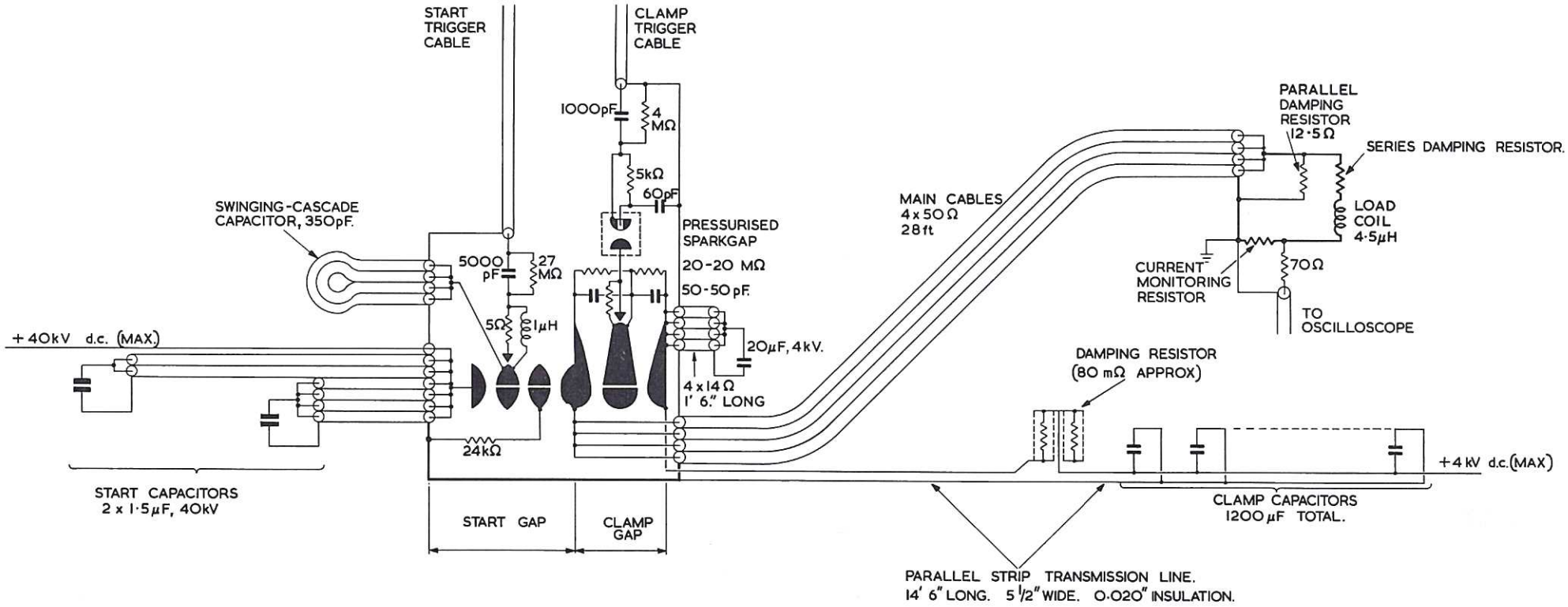

Fig. 8 (CLM-P 127)
Details of the final powered-clamp discharge circuit

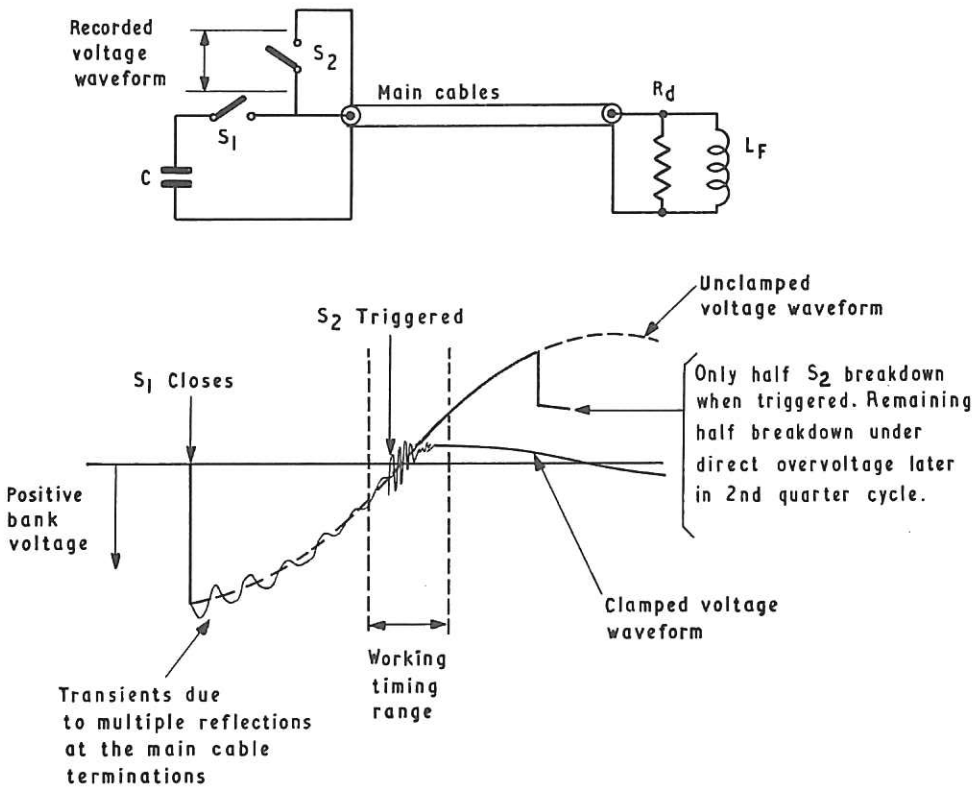

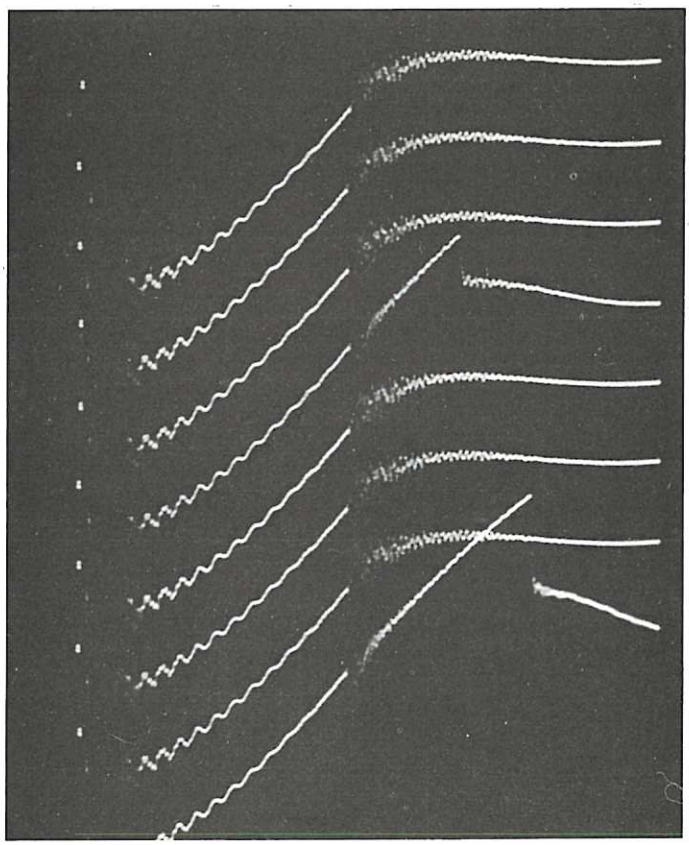

Fig. 9 (CLM-P 127)
Voltage waveforms measured across the clamp spark gap

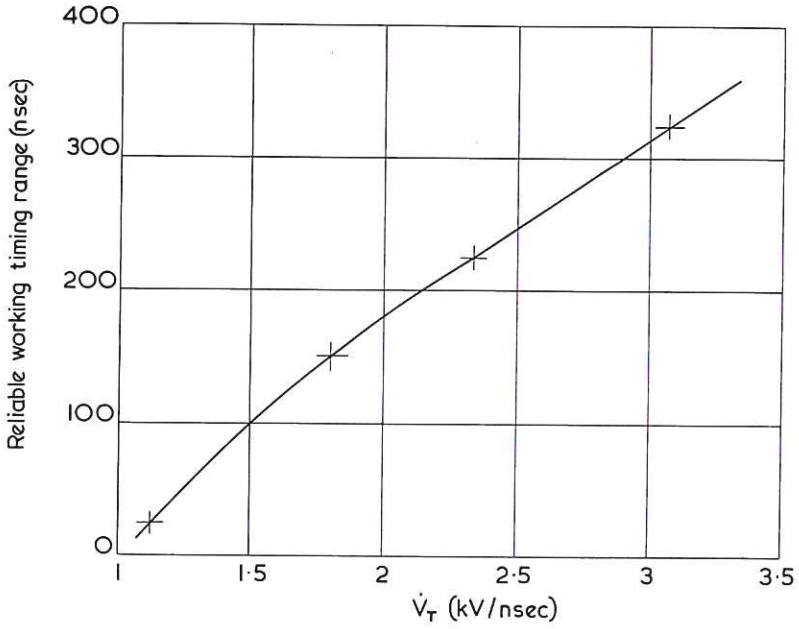

Fig. 10 Graph : timing range - vs - $\dot{V}_T$ (CLM-P 127)

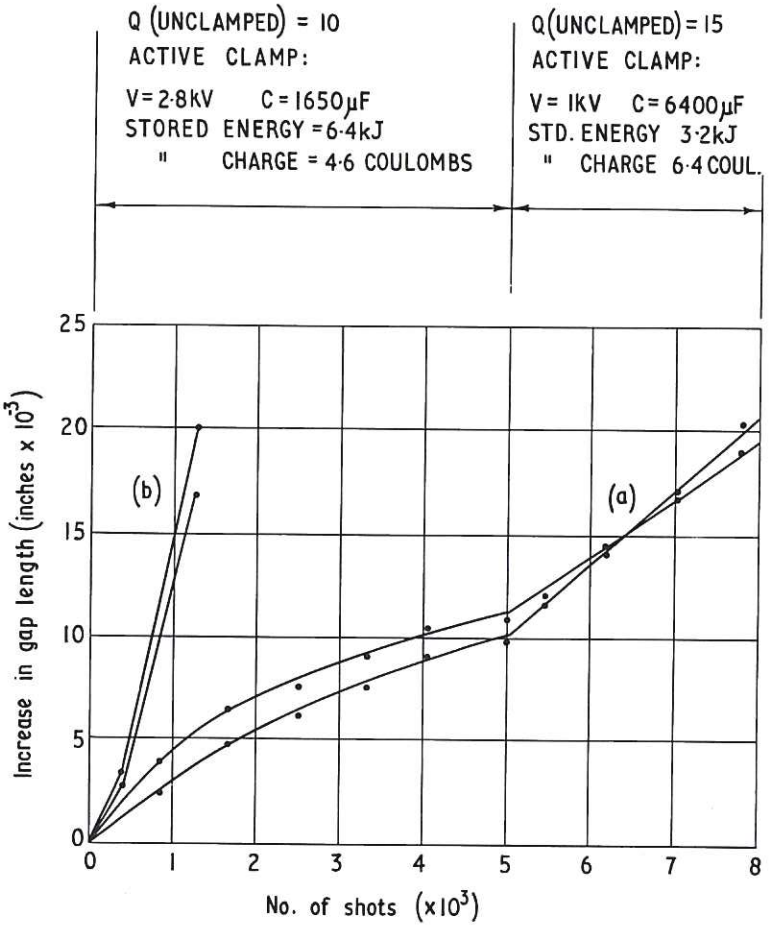

(a) PEAR-SHAPED ELECTRODES: MAGNETIC BLOW-OUT.

(b) HEMISPHERICAL ELECTRODES: NO MAGNETIC BLOW-OUT.

Fig. 11 (CLM-P 127)

Graph : increase in gap lengths - vs - number of shots with and without magnetic blowout of the arc

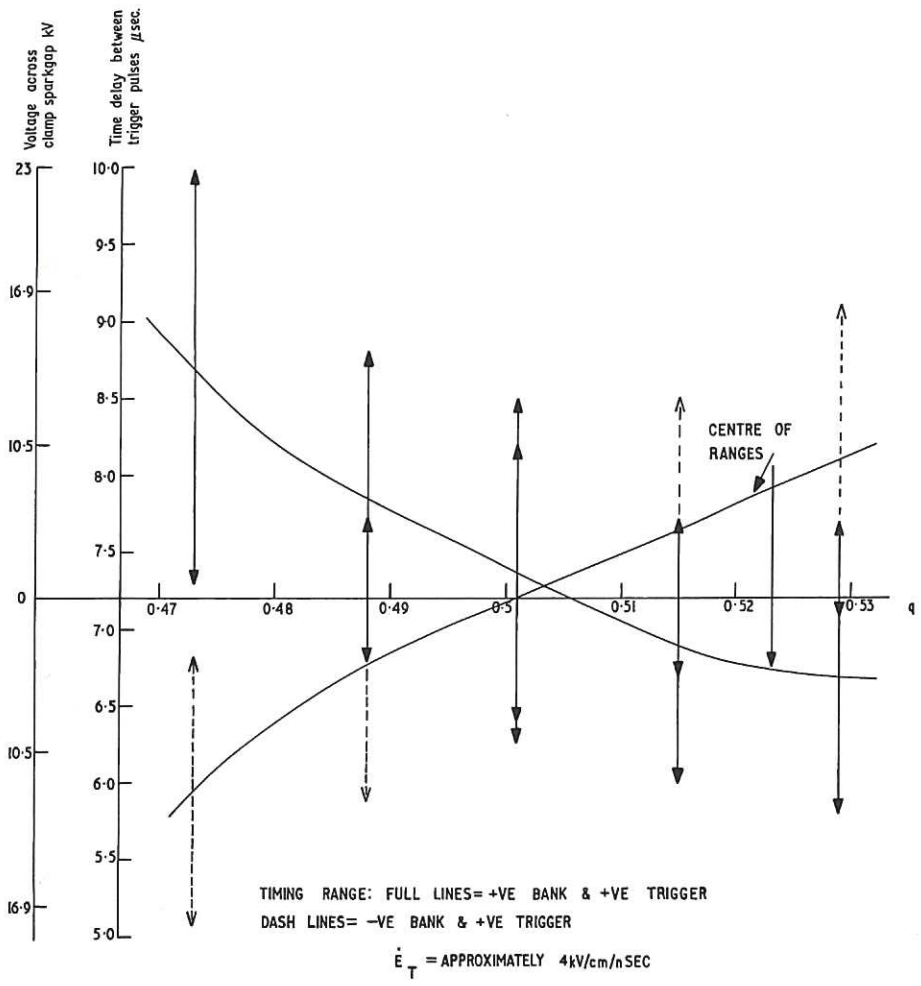

Fig. 12 (CLM-P 127)
Graph: timing range - vs - gap ratio q

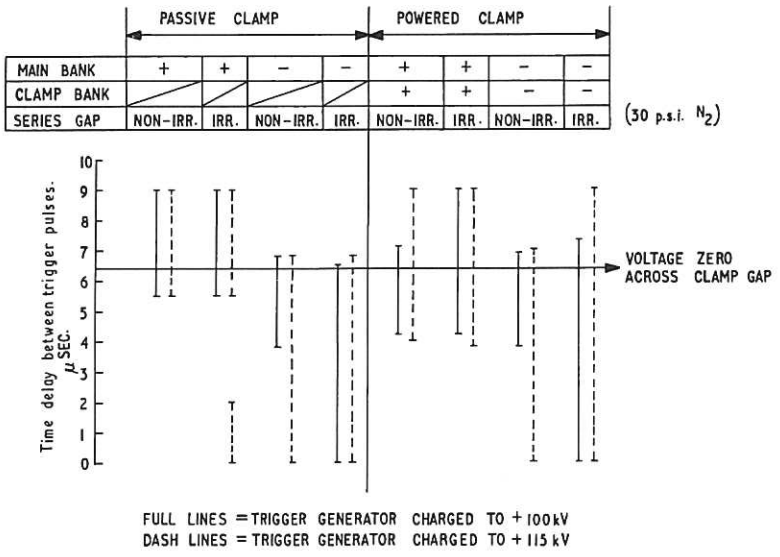

Fig. 13 (CLM-P 127)
Graph: timing range measurements on one circuit of the powered-clamp test rig

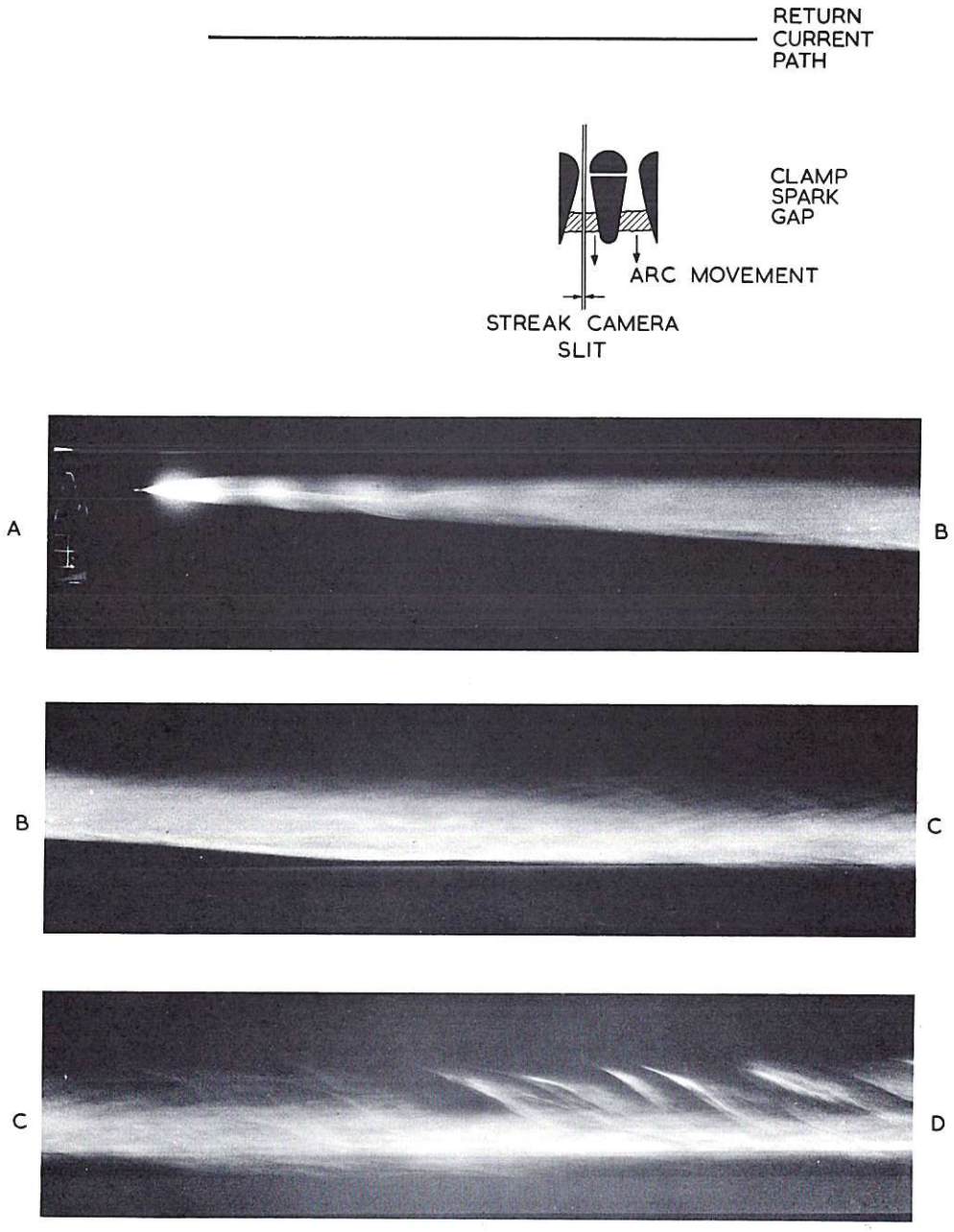

Fig. 14 Streak-camera record (CLM-P 127)

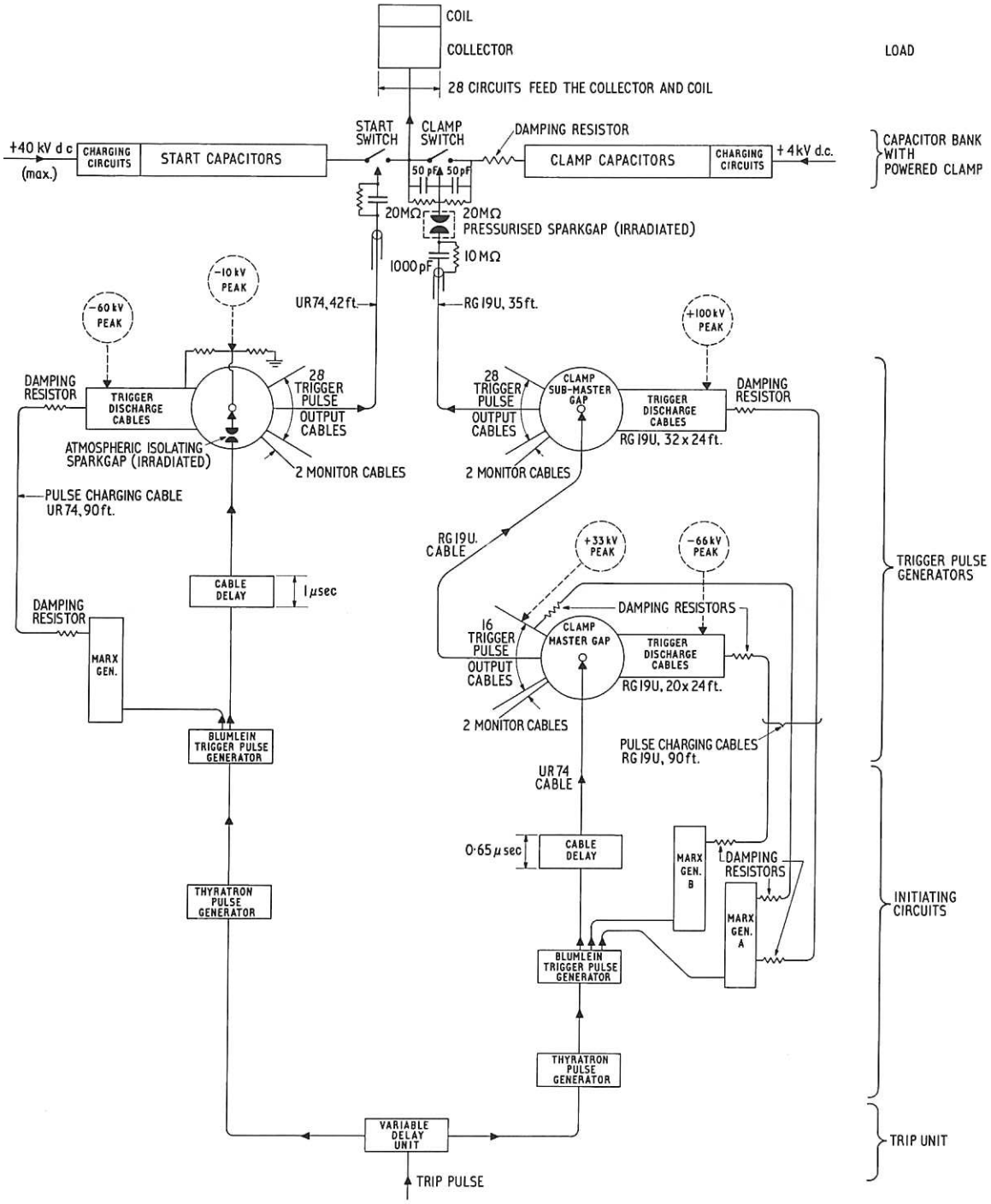

Fig. 15 (CLM-P 127)
Schematic diagram of the powered-clamp test rig

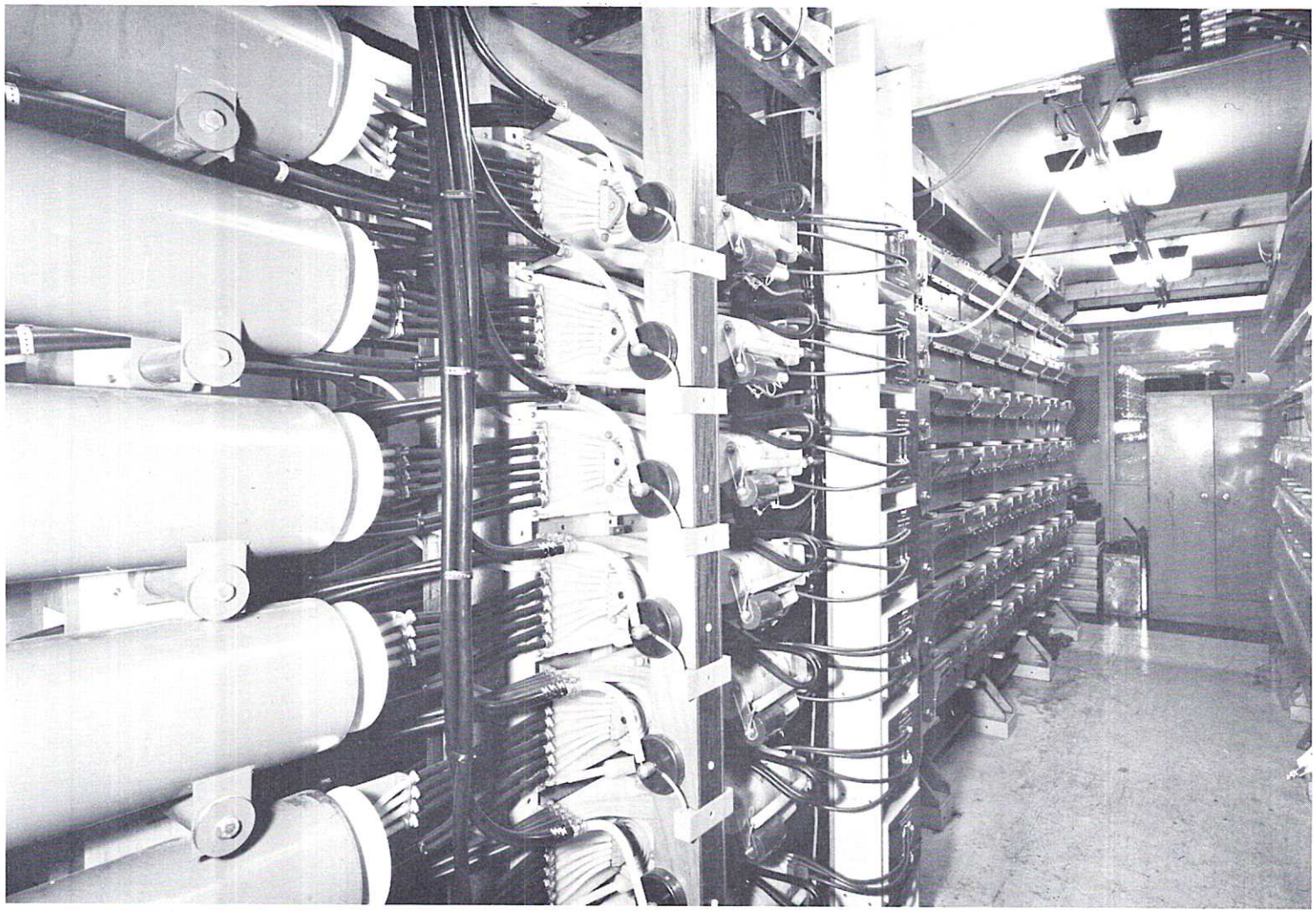

Fig. 16 (CLM-P 127)
Photograph : view between racks of test rig from the start-capacitor end

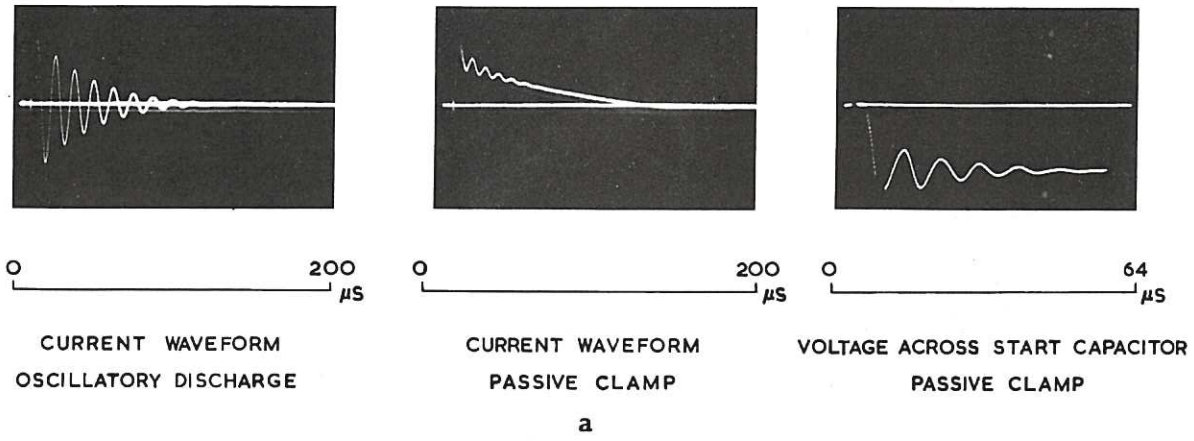

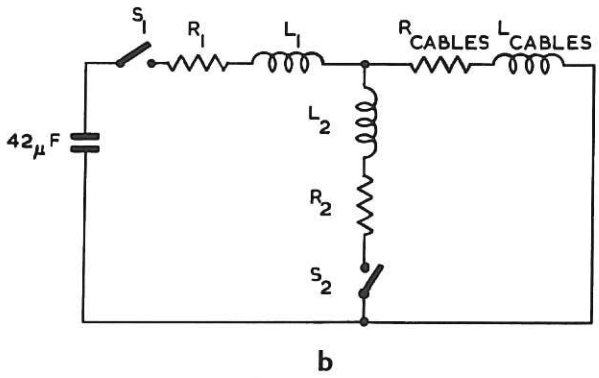

Fig. 17 (CLM-P 127)
The discharge of one rack of the test rig into a short circuit
(a) waveforms: (b) equivalent circuit

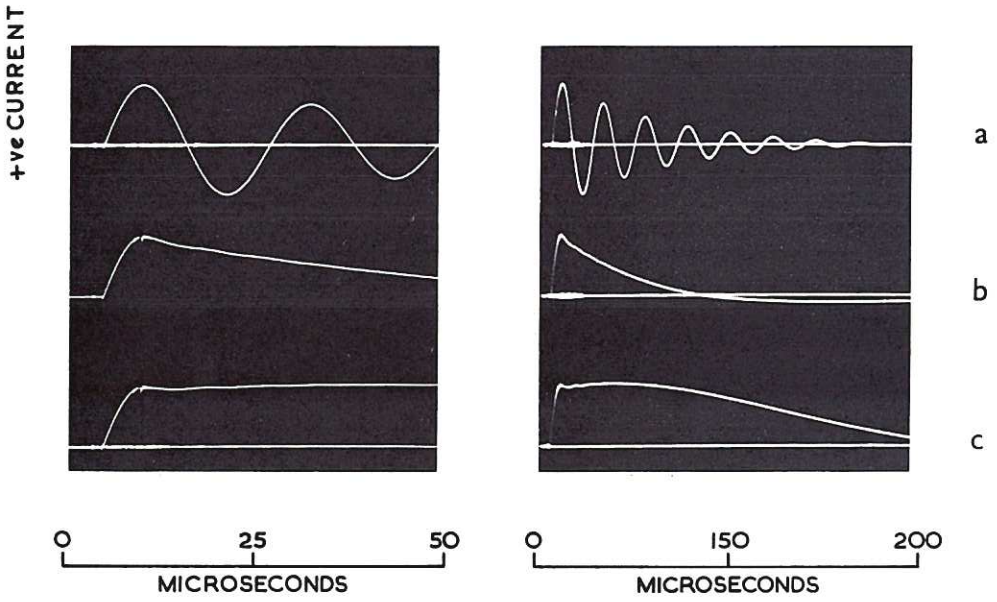

a

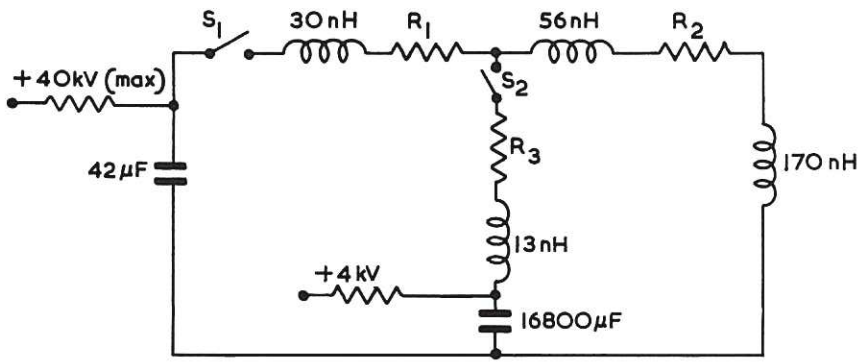

b

Fig. 18 (CLM-P 127)

Current waveforms produced by one rack discharging into a 170-nanohenry load coil
(a) unclamped: (b) passive clamp: (c) powered clamp

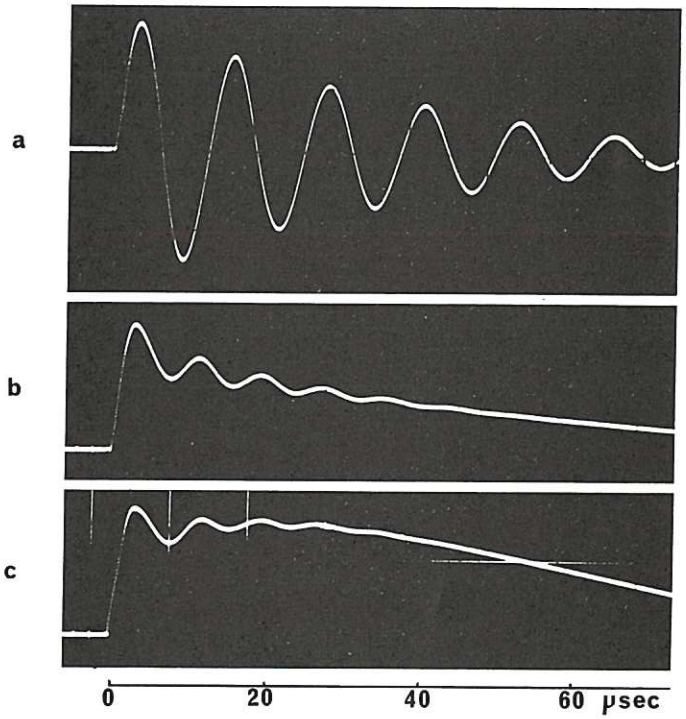

Fig. 19 (CLM-P 127)
Current waveforms produced by two racks discharging into a 20-nanohenry thetatron coil